

Adaptive Nonlinear States Observer Design of Switched Reluctance Machine

ALI BOUKLATA¹, SARA BARBARA¹, MOHAMED BENYASSI², HAFID OUBOUADDI¹,
CHAIMAE ABDELAALI¹, ADIL BROURI¹

¹AEED Department, ENSAM,
Moulay Ismail University,
MOROCCO

²Electrical Engineering Department, ESTM,
Moulay Ismail University,
MOROCCO

Abstract: - This paper presents an adaptive nonlinear observer designed for switched reluctance machines (SRMs). In this study, a diffeomorphism transformation was performed to reformulate the system into an observable form, and then a Kalman high-gain observer (KHGO) was developed to online estimate the electrical and mechanical parameters of the machine. The performance of the observer is confirmed through simulations carried out using MATLAB/Simulink environment under various scenarios. The results confirmed its ability to accurately estimate the electromechanical states of the machine for different operating conditions.

Key-Words: - Switched Reluctance Machine (SRM), Adaptive Nonlinear Observer, State Estimation, Sensorless Control, Kalman-High-Gain Observer, State-Space Model, Triangular Form Observable.

Received: July 9, 2024. Revised: December 29, 2024. Accepted: February 23, 2025. Published: April 30, 2025.

1 Introduction

The use of switched reluctance machines in different industrial applications, particularly electric vehicles (EVs) and hybrid electric vehicles (HEVs), is becoming very frequent due to their robust design, absence of permanent magnets, and torque-speed characteristics, [1], [2], [3], [4], [5]. Their capability to ride through faults provides enhanced safety and reliability that renders them particularly good for applications plagued by the high cost of rare-earth magnets, [6], [7], [8]. Despite the advantages, SRMs have significant control-related problems because they feature a complex control system with nonlinear measures that prevented them from being operated in the open loop. Furthermore, there are some other issues, including torque ripples and acoustic noise, that complicate the control approach, [9], [10].

One of the prime problems is sensorless control which seeks to use fewer measurements to reduce the use of physical sensors and has been studied through several approaches such as sliding mode observers and the extended Kalman filter, [11], [12].

Existing sensorless control methods for SRM face notable limitations, particularly in maintaining

accuracy across varying speed ranges and their sensitivity to model simplifications. It is demonstrated that the Luenberger observer performs well at medium to high speeds but struggles with starting hesitation and zero-speed observability, [13]. A high-gain Kalman-like observer is developed to enhance rotor position and speed reconstruction from electrical measurements. However, it faces constraints related to non-uniform observability and requires constant-speed inputs, [14]. An Extended Kalman Filter and Second Order Sliding Mode Observer were employed to estimate rotor position, velocity, and unknown load torque, demonstrating reliability in simulations but being limited to simulated environments, [12]. [15], addresses the challenge of state observation for sensorless control by deriving algebraic relations between unknown rotor flux and measured quantities, using adaptive nonlinear observers. Their approach addresses various mathematical models of SRM and demonstrates effectiveness through simulations with a finite element model. Despite these advancements, challenges related to observability, starting hesitation, and varying operational conditions continue to hinder the

development of universally applicable sensorless control methods.

This paper introduces a novel technique that employs a nonlinear observer for the simultaneous estimation of states in SRM. Our key contribution lies in the diffeomorphism transformation of the SRM model into an observable form in the z-coordinates, [16]. This transformation enables the application of a Kalman high-gain observer, [17], which is specifically designed to handle the unique characteristics of SRM. After applying the observer, we perform an inverse transformation to obtain the observer in the original x-coordinates. This method not only improves robustness and accuracy in sensorless control but also effectively addresses the challenges posed by the motor's commutation stages and the non-uniform observability conditions. Our approach overcomes the limitations of existing methods, particularly their applicability across varying speed ranges and sensitivity to model simplifications, offering a more reliable and efficient solution for SRM control. The effectiveness of the proposed scheme is confirmed through inclusive simulations.

The remainder of this paper is organized as follows. In Section 2, we present the SRM model and its commutation processes, including four mathematical models. Section 3 relies on the nonlinear observer design for SRMs, detailing the observability analysis and the development of the proposed observer. Section 4 introduces the numerical simulations, providing results that validate the proposed method. Finally, Section 5 exhibits some concluding remarks as well discusses future research directions.

2 System Modeling

SRMs are distinguished by their simple and robust design, lack of rotor windings or permanent magnets, and their ability to operate across a wide speed range. This section details the modeling of SRM, focusing on the fundamental principles and mathematical formulations that describe their behavior.

In this section, we present the mathematical modeling of the SRM, including the fundamental equations governing its electrical and mechanical dynamics. The model encompasses the relationship between the phase inductances, currents, and the resultant electromagnetic torque. It also accounts for the non-linear characteristics inherent in SRM, such as the dependence of inductance on rotor position and current.

$$\frac{di}{dt} = \frac{1}{L(\theta)} \left(-\omega \frac{dL(\theta)}{d\theta} i - R i + u \right) \quad (1a)$$

$$\frac{d\theta}{dt} = \omega \quad (1b)$$

$$\frac{d\omega}{dt} = \frac{1}{2J} i \frac{dL(\theta)}{d\theta} i^T - \frac{F}{J} \omega - \frac{T_L}{J} \quad (1c)$$

$$\frac{dT_L}{dt} = w(t) \quad (1d)$$

where θ represent the rotor position, ω the angular velocity, i the phases current, $L(\theta)$ the phases inductance, R the phases resistance, u the phase voltage, and J the moment of inertia of the rotor.

$$i = [i_1 \ i_2 \ i_3]^T, L(\theta) = \begin{bmatrix} L_1(\theta) & 0 & 0 \\ 0 & L_2(\theta) & 0 \\ 0 & 0 & L_3(\theta) \end{bmatrix},$$

$$R = \begin{bmatrix} R_1 & 0 & 0 \\ 0 & R_2 & 0 \\ 0 & 0 & R_3 \end{bmatrix}, u = [u_1 \ u_2 \ u_3]^T$$

In this study, unlike the approach taken in [18], we consider non-saturated winding inductances, which are characterized by:

$$L(\theta) = \begin{cases} L_u & \theta_1 < \theta < \theta_2 \\ L_u + M\theta & \theta_2 < \theta < \theta_3 \\ L_a & \theta_3 < \theta < \theta_4 \\ L_u - M\theta & \theta_4 < \theta < \theta_5 \\ L_u & \theta_5 < \theta < \theta_6 \end{cases}; M = \frac{L_a - L_u}{\alpha}$$

α , L_u and L_a is the pole arc of stator the minimum inductance and the maximum inductance respectively.

Assumption 1. The parameters of the system (J , F and R) are known, but the function $w(t)$ is bounded and is not known.

2.1 State Space Representation

As the SRM phases are excited independently, the analysis and design can be performed by considering each phase separately and identifying the active phase. adopting the following notations:

$\beta(\theta) = \frac{1}{L(\theta)}$; $\gamma(\theta) = \frac{dL(\theta)}{d\theta}$; $x = [x_1 \ x_2 \ x_3 \ x_4]^T = [i \ \theta \ \omega \ T_L]^T$ the space-state model given (1) is redefined as follows:

$$\dot{x}_1 = \beta(x_2)(-x_3\gamma(x_2)x_1 - Rx_1 + u) \quad (2a)$$

$$\dot{x}_2 = x_3 \quad (2b)$$

$$\dot{x}_3 = \frac{1}{2J}x_1^2\gamma(x_2) - \frac{F}{J}x_3 - \frac{1}{J}x_4 \quad (2c)$$

$$\dot{x}_4 = w(t) \quad (2d)$$

Let take: $\bar{u} = -Rx_1 + u$

$$\dot{x}_1 = \beta(x_2)(-x_3\gamma(x_2)x_1 + \bar{u}) \quad (3a)$$

$$\dot{x}_2 = x_3 \quad (3b)$$

$$\dot{x}_3 = \frac{1}{2J}x_1^2\gamma(x_2) - \frac{F}{J}x_3 - \frac{1}{J}x_4 \quad (3c)$$

$$\dot{x}_4 = w(t) \quad (3d)$$

$$y(t) = x_3 \quad (3e)$$

In the extended representation of the state space, the system model (3) is described as follows:

$$\dot{x} = f(x) + g(x)\bar{u} + Dw(t) \quad (4a)$$

$$y = h(x) \quad (4b)$$

f, g and h are expressed as follows:

$$f = \begin{bmatrix} -\beta(x_2)\gamma(x_2)x_1x_3 \\ x_3 \\ ax_1^2\gamma(x_2) - \frac{F}{J}x_3 - cx_4 \\ 0 \end{bmatrix} \quad (5)$$

$$g = [\beta(x_2) \ 0 \ 0 \ 0]^T, D = [0 \ 0 \ 0 \ 1]^T \quad (6)$$

$$h(x) = x_3 \quad (7)$$

3 SRM Nonlinear Observer Design

3.1 Transformation of the SRM Nonlinear Model in a Nonlinear Canonical Observer Form

The nonlinearity and lack of a canonical form of the initial SRM model (4)-(5) make it unsuitable for observer design. Therefore, the first step involves turning it into a canonical observer form. This process is addressed in the following proposition:

Proposition 1. A Lipschitzian diffeomorphism is presented:

$$T(x): \mathbb{R}^4 \rightarrow \mathbb{R}^4, x \rightarrow z = \begin{bmatrix} z_1 \\ z_2 \\ z_3 \\ z_4 \end{bmatrix} = T(x) = \begin{bmatrix} T_1(x) \\ T_2(x) \\ T_3(x) \\ T_4(x) \end{bmatrix} \quad (8)$$

The system (4)–(5) is subsequently transformed to the following canonical form:

$$\dot{z}(t) = Az(t) + g(z(t), \bar{u}) + Bw(t)\varphi(z) \quad (9a)$$

$$y(t) = Cz(t) \quad (9b)$$

$$\text{With: } A = \begin{bmatrix} 0 & 1 & 0 & 0 \\ 0 & 0 & 1 & 0 \\ 0 & 0 & 0 & 1 \\ 0 & 0 & 0 & 0 \end{bmatrix}, C = [1 \ 0 \ 0 \ 0]$$

$$g(z, u) = \begin{bmatrix} g_1(z_1, u) \\ g_2(z_1, z_2) \\ g_3(z_1, z_2, z_3) \\ g_4(z, u) \end{bmatrix}, B = [0 \ 0 \ 0 \ 1]$$

where $g_1 \in \mathbb{R}^2, g_2 \in \mathbb{R}^2, g_3 \in \mathbb{R}^2$ and $g_4 \in \mathbb{R}^2$

Proof of Proposition 1. In order to obtain the canonical form given in (9), we are applying the

method developed in [19]. The degree of the system is 4 while the relative degree is 2, so we pose the transformation by derivation of the following lees:

$$z = T(x) = [\ \emptyset(x) \ \mu(x) \ h(x) \ L_f h(x)]^T \quad (10)$$

We select $\emptyset(x)$ in which T is a diffeomorphism, i.e.:

$$\frac{\partial \emptyset(x)}{\partial x} g(x) = 0 \quad (11a)$$

$$\left[\frac{\partial \emptyset(x)}{\partial x_1} \ \frac{\partial \emptyset(x)}{\partial x_2} \ \frac{\partial \emptyset(x)}{\partial x_3} \ \frac{\partial \emptyset(x)}{\partial x_4} \right] \begin{bmatrix} \beta(x_2) \\ 0 \\ 0 \\ 0 \end{bmatrix} = 0 \quad (11b)$$

$$\frac{\partial \emptyset(x)}{\partial x_1} \beta(x_2) = 0 \quad (11c)$$

$$\frac{\partial \emptyset(x)}{\partial x_1} = 0 \quad (11d)$$

Thus, if $\emptyset(x)$ does not depend on x_1 we can:

$$\text{choose } \emptyset(x) = x_2 \quad (12)$$

We choose $\mu(x)$ such that T is a diffeomorphism, meaning that:

$$\frac{\partial \mu(x)}{\partial x} g(x) = 0 \quad (13a)$$

$$\left[\frac{\partial \mu(x)}{\partial x_1} \ \frac{\partial \mu(x)}{\partial x_2} \ \frac{\partial \mu(x)}{\partial x_3} \ \frac{\partial \mu(x)}{\partial x_4} \right] \begin{bmatrix} \beta(x_2) \\ 0 \\ 0 \\ 0 \end{bmatrix} = 0 \quad (13b)$$

$$\frac{\partial \mu(x)}{\partial x_1} \beta(x_2) = 0 \quad (13c)$$

$$\frac{\partial \mu(x)}{\partial x_1} = 0 \quad (13d)$$

Thus, if $\mu(x)$ does not depend on x_1 we can choose $\mu(x) = x_4 + x_3$ (14)

Then we calculate $L_f h(x)$

$$L_f h(x) = \left[\frac{\partial h(x)}{\partial x_1} \ \frac{\partial h(x)}{\partial x_2} \ \frac{\partial h(x)}{\partial x_3} \ \frac{\partial h(x)}{\partial x_4} \right] f(x) = \frac{1}{2J} x_1^2 \gamma(x_2) - \frac{F}{J} x_3 - cx_4 \quad (15)$$

We obtain the following transformation:

$$z = [z_1 \ z_2 \ z_3 \ z_4]^T = T(x) = [x_2 \ x_4 + x_3 \ x_3 \ L_f h(x)]^T \quad (16)$$

$$\dot{z}_1 = \dot{x}_2 = x_3 = z_2 \quad (17a)$$

$$\dot{z}_2 = \dot{x}_4 + \dot{x}_3 = w(t) + z_3$$

$$\dot{z}_3 = \dot{x}_3 = \frac{1}{2J} x_1^2 \gamma(x_2) - \frac{F}{J} x_3 - cx_4 = z_4 \quad (17b)$$

$$\dot{z}_4 = \frac{1}{J} x_1 \dot{x}_1 \gamma(x_2) + \frac{1}{2J} x_1^2 \dot{x}_2 \frac{d\gamma}{dx_2} - \frac{F}{J} z_3 - cz_4 = \frac{1}{J} x_1 \dot{x}_1 \gamma(x_2) - \frac{F}{J} z_3 - cw(t) \quad (17c)$$

$$\dot{z}_4 = -\beta(x_2)\gamma(x_2)x_1x_3 \left(\frac{1}{2J} x_1 \dot{x}_1 \gamma(x_2) \right) \frac{F}{J} z_3$$

$$-\frac{F}{J}\left(\frac{1}{2J}x_1^2\gamma(x_2) - \frac{F}{J}x_3 - c x_4\right) \quad (17d)$$

We have $\frac{d\gamma}{dx_2} = 0$, This gives us the following triangular model:

$$\dot{z}_1 = z_2 \quad (18a)$$

$$\dot{z}_2 = w(t) + z_3 \quad (18b)$$

$$\dot{z}_3 = z_4 \quad (18c)$$

$$\dot{z}_4 = -\beta(x_2)\gamma(x_2)x_1x_3 \left(\frac{1}{2J}x_1\dot{x}_1\gamma(x_2)\right)\frac{F}{J}z_3 \quad (18d)$$

$$y = z_2 \quad (18e)$$

It is clear that the model of the system described in equation (18) has a triangular structure, which represents a canonical form of observability. This model can be expressed in the following concise form:

$$\dot{z}(t) = Az(t) + g(z(t), \bar{u}) + Bw(t)\varphi(z) \quad (19a)$$

$$y = Cz = z_2 \quad (19b)$$

With: $A = \begin{bmatrix} 0 & 1 & 0 & 0 \\ 0 & 0 & 1 & 0 \\ 0 & 0 & 0 & 1 \\ 0 & 0 & 0 & 0 \end{bmatrix}, \quad C = [0 \ 1 \ 0 \ 0]$

$$g(z) = \begin{bmatrix} 0 \\ 0 \\ 0 \\ v(z) \end{bmatrix}, \quad \varphi(z) = \begin{bmatrix} 0 \\ 1 \\ 0 \\ 0 \end{bmatrix}, \quad B = \begin{bmatrix} 0 \\ 1 \\ 0 \\ 0 \end{bmatrix}$$

$$v(z) = -\beta(x_2)\gamma(x_2)x_1x_3 \left(\frac{1}{2J}x_1\dot{x}_1\gamma(x_2)\right)\frac{F}{J}z_3 \quad (20)$$

3.2 Observer Design of the SRM in the z-Coordinates

We proceed by considering the following High-Gain-Kalman Design, like in [20].

$$\dot{\hat{z}} = A\hat{z} + g(\hat{z}, u) + \Delta(K)P^{-1}C^T(y - C\hat{z}) \quad (21a)$$

In (21) the observer matrix $\Delta(K)$ and P are defined as following:

$$\Delta(K) = \begin{bmatrix} K & 0 & 0 \\ 0 & K^2 & 0 \\ 0 & 0 & K^3 \end{bmatrix} \quad (21b)$$

$$\dot{P} = K(-\lambda P - A^T P - P A + C^T C) \quad (21c)$$

The gain k and λ are selected based on the following assumptions:

Assumption 2. for any positive definite matrix P_0 , there exist positive scalars K^* , α_1 and α_2 such that for any $K \geq K^*$, any $\lambda \geq 2A_{max}$ and any initial condition $z_0 \in \mathbb{R}^{dz}$, the matrix differential equation initialized at $P(0) = P_0$ has a unique solution which

satisfies $P(t)^T = P(t)$ for all t and $\alpha_1 I < P(t) < \alpha_2 I \ \forall t \geq \frac{1}{L}$.

3.3 The SRM Observer Design in the x-Coordinates

In the previous subsection, the state observer for the system (4) was developed using z -coordinates. For practical implementation, however, it is required to express this observer in x -coordinates. The process of converting the dynamics of state variables in z -coordinates and x -coordinates is facilitated through the relationships outlined in Eqs. (8) and (9). By applying the diffeomorphism transformation $z = T(x)$, we can derive the derivative of the estimated state in x -coordinates as follows:

$$\frac{d\hat{z}}{dt} = \frac{dT(\hat{x})}{d\hat{x}} \frac{d\hat{x}}{dt} = \Gamma \frac{d\hat{x}}{dt} \quad (22)$$

$$\dot{\hat{z}}(t) = \Gamma \dot{\hat{x}}(t) \Rightarrow \dot{\hat{x}}(t) = \Gamma^{-1} \dot{\hat{z}}(t) \quad (23)$$

$$\dot{\hat{x}}(t) = \Gamma^{-1}[A\hat{z} + g(\hat{z}, u) + \Delta(K)P^{-1}C^T(y - C\hat{z})] \quad (24)$$

$$\dot{\hat{x}}(t) = f(\hat{x}, u) + \Delta(K)P^{-1}\Gamma^{-1}C^T(x - \hat{x}) \quad (25)$$

4 Numerical Simulations

This section presents the results of numerical simulations conducted to assess the adaptive nonlinear observer's performance developed for the SRM. The simulations were carried out using MATLAB/Simulink environments to demonstrate the robustness and efficiency of the observer under various operating conditions.

The machine used in the simulations has the following characteristics in Table 1.

Table 1. SRM parameters

Parameter	Symbol	Value
Rotational speed	ω_m	1500 RPM
Stator resistance	R_s	0.01Ω
Stator poles number	N_s	6
Rotor poles number	N_r	4
Maximal inductance	L_{max}	23.6 mH
Minimal inductance	L_{min}	0.67 mH
Nominal power	P	1,5 Kw

Figure 1, Figure 2, and Figure 3 illustrate the observer's response to variations in rotor speed across three different states. Figure 1 shows the current and its estimate, it can be seen that the current is well tracked by the observer. Figure 1 shows the current and its estimate; it can be seen that the current is well tracked by the observer.

Figure 2 shows the rotor position and its estimation, showing the high precision of the estimation. Figure 3 presents the rotor speed and its estimation; the rotor speed estimation error is very low even when there is large variation in the speed, proving the robustness and fast convergence of the observer.

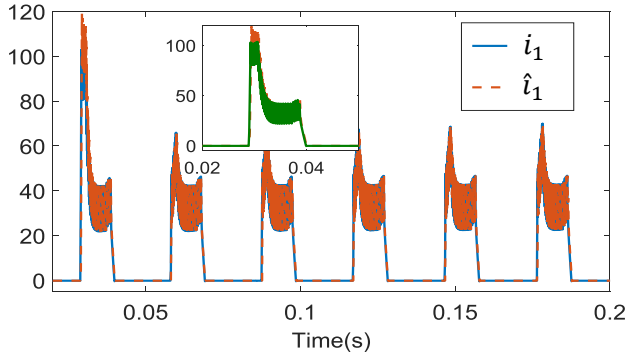


Fig. 1: Current i_1 (dashed) and its estimate \hat{i}_1 (solid)

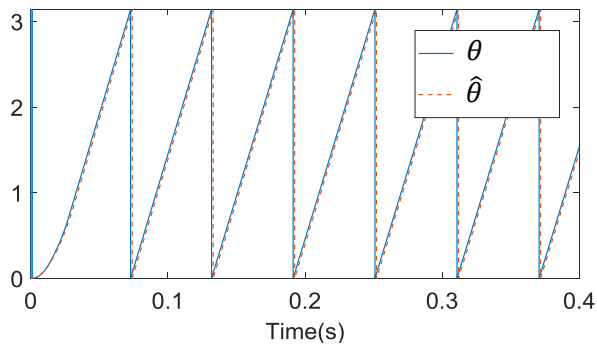


Fig. 2: Rotor position θ (dashed) and its estimate $\hat{\theta}$ (solid)

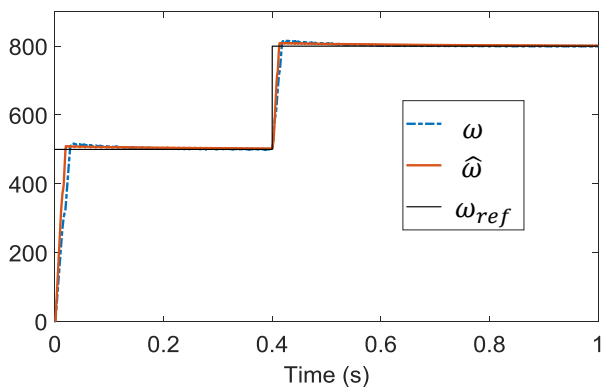


Fig. 3: Rotational speed ω (dashed) and its estimate $\hat{\omega}$ (solid)

Figure 4, Figure 5 and Figure 6 show the evolution of the measured rotor speed and its estimation as a function of time under varying load conditions. Figure 4 illustrates the effect of load

variation on the performance of the proposed observer at time $t=0.4s$. Figure 5 shows the increase in current value with load and the convergence to zero of the estimation error. Figure 6 confirms that the estimation error of the rotor position remains minimal even with load variations, which highlights the robustness of the observer. Overall, these figures demonstrate that the designed observer provides accurate state estimation under varying load conditions.

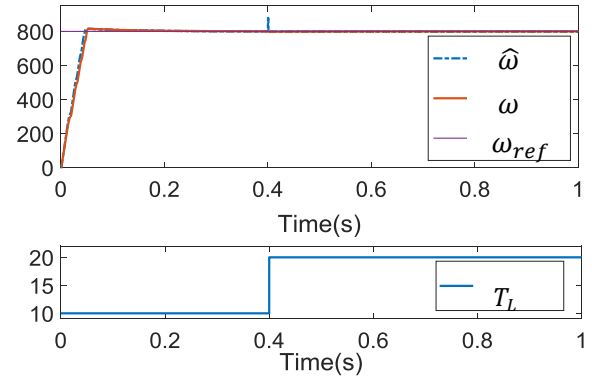


Fig. 4: Rotational speed ω (dashed) and its estimate $\hat{\omega}$ (solid) under variable load

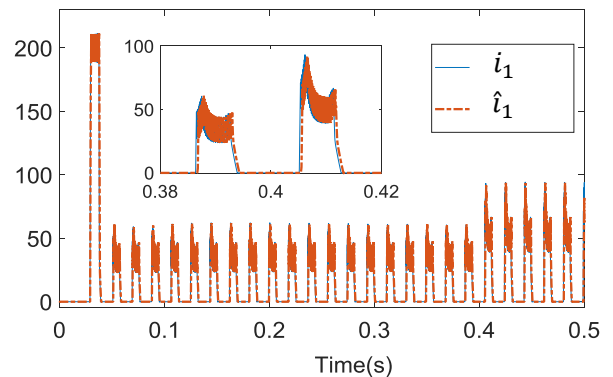


Fig. 5: Current i_1 (dashed) and its estimate \hat{i}_1 (solid)

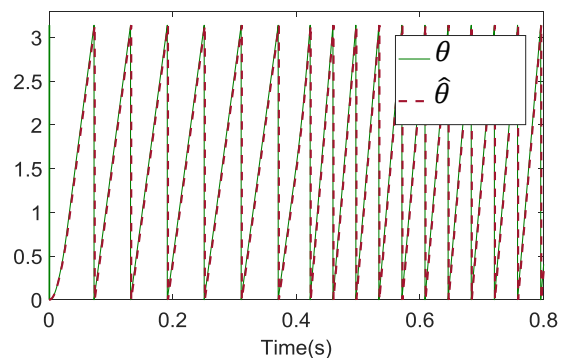


Fig. 6: Rotor position θ (dashed) and its estimate $\hat{\theta}$ (solid)

The simulation results highlight the excellent performance of adaptive non-linear observation under different operating conditions. This is illustrated by its low estimation error and its ability to adapt quickly to variations in load and speed.

5 Conclusion

In this work, an adaptive nonlinear observer has been proposed for an SRM to guarantee state estimation. Thanks to a detailed observability analysis and a diffeomorphism transformation into an observable form, we were able to implement the observer. Simulation results confirmed the developed observer's performance, which showed that SRM states were accurately reconstructed, thus improving machine control without the need for additional sensors.

References:

- [1] L. Kadi, A. Brouri, A. Ouannou, K. Lahdachi, Modeling and Determination of Switched Reluctance Machine Nonlinearity, *IEEE Conference on Control Technology and Applications (CCTA)*, Montreal, QC, Canada, Aug 24-26, pp. 898-902, 2020.
- [2] A. Bouklata, H. Oubouaddi, A. Brouri, M.I. Mosaad, F. Giri, "Advanced Control Strategy of Switched Reluctance Generator-Based Wind Energy Conversion Systems Using Backstepping and Extremum Seeking Techniques," *IFAC-PapersOnLine*, vol. 58, no. 13, pp. 593-598, 2024.
- [3] H. Oubouaddi, A. Brouri, A. Ouannou, A. Bouklata, F.E. El Mansouri, "Feedback Linearization Technique for Speed and Torque Control of Switched Reluctance Machine," *E3S Web of Conferences*, vol. 469, p. 00058, 2023.
- [4] T.A.D.S. Barros, P.J.D.S. Neto, M.V. De Paula, A.B. Moreira, P.S. Nascimento Filho, E. Ruppert Filho, Automatic characterization system of switched reluctance machines and nonlinear modeling by interpolation using smoothing splines, *IEEE Access*, vol. 6, pp. 26011-26021, 2018.
- [5] F.E. El Mansouri, M.I. Mosaad, L. Kadi, A. Ouannou, H. Oubouaddi, A. Brouri, "Application of Frequency Response Analysis for Parameters Estimation of Switched Reluctance Motors," *Journal of Electrical Engineering & Technology*, vol. XX, no. X, pp. 1-21, 2024.
- [6] A. Brouri, L. Kadi, A. Tounzi, A. Ouannou, J. Bouchnaif, Modelling and identification of switched reluctance machine inductance, *Australian Journal of Electrical and Electronics Engineering*, Taylor & Francis, vol. 18, no. 1, pp. 8-20, 2020.
- [7] A. Ouannou, A. Brouri, F. Giri, L. Kadi, H. Oubouaddi, S.A. Hussien, N. Alwadai, M.I. Mosaad, Parameter Identification of Switched Reluctance Motor SRM Using Exponential Swept-Sine Signal, *Machines*, *MDPI*, vol. 11, no. 625, pp. 1-15, 2023.
- [8] C. Gan, Y. Chen, R. Qu, Z. Yu, W. Kong, Y. Hu, An overview of fault-diagnosis and fault-tolerance techniques for switched reluctance machine systems, *IEEE Access*, vol. 7, pp. 174822-174838, 2019.
- [9] H. Abdelmaksoud, S. Shaaban, Torque Ripple Reduction in SR Motor Operating without Rotor Position Sensor, *Advances in Electrical and Computer Engineering*, vol. 22, no. 3, pp. 53-60, 2022.
- [10] Y. Hu, C. Gu, Z. Zhang, Z. Kang, Y. Li, Torque Ripple Minimization of Six-Phase Switched Reluctance Motor Based on Enhanced Direct Instantaneous Torque Control, *IEEE Transactions on Transportation Electrification*, IEEE, 2023.
- [11] X. Li, J. Liu, L. Ge, J. Zhong, J. Huang, Y. Zhao, S. Song, Sensorless control of the switched reluctance motor based on the sliding-mode observer, *Journal of Electrical Engineering & Technology*, Springer, vol. 18, no. 2, pp. 981-989.
- [12] Y. Saadi, R. Sehab, A. Chaibet, M. Boukhniher, D. Diallo, Sensorless control of Switched Reluctance Motor with unknown load torque for EV application using Extended Kalman Filter and second order sliding mode observer, *IEEE International Conference on Industrial Technology (ICIT)*, Lyon, France, Feb 20-22, pp. 522-528, 2018.
- [13] P. Brandstetter, O. Petrtlyl, J. Hajovsky, Luenberger observer application in control of switched reluctance motor, *International Scientific Conference on Electric Power Engineering (EPE)*, IEEE, Prague, Czech Republic, May 18-20, pp. 1-5, 2016.
- [14] A. de La Guerra, A.G. Giles, G. Besançon, Immersion based observer for the switched reluctance motor, *IFAC-PapersOnLine*, Elsevier, vol. 53, no. 2, pp. 5934-5939, 2020.
- [15] R. Ortega, A. Sarr, A. Bobtsov, I. Bahri, D. Diallo, Adaptive state observers for sensorless control of switched reluctance motors,

International Journal of Robust and Nonlinear Control, Wiley, vol. 29, no. 4, pp. 990-1006, 2019.

- [16] D. Boutat, K. Busawon, On the transformation of nonlinear dynamical systems into the extended nonlinear observable canonical form, *International Journal of Control*, Taylor & Francis, vol. 84, no. 1, pp. 94-106, 2011.
- [17] S. Bououden, D. Boutat, G. Zheng, J.P. Barbot, F. Kratz, A triangular canonical form for a class of 0-flat nonlinear systems, *International Journal of Control*, Taylor & Francis, vol. 84, no. 2, pp. 261-269, 2011.
- [18] H.E. Abdel-Maksoud, M.M. Khater, S.M. Shaaban, Adaptive Fuzzy Logic PI Control for Switched Reluctance Motor Based on Inductance Model, *International Journal of Intelligent Engineering & Systems*, vol. 10, no. 4, 2017.
- [19] H.K. Khalil, L. Praly, High-gain observers in nonlinear feedback control, *International Journal of Robust and Nonlinear Control*, Wiley, vol. 24, no. 6, pp. 993-1015, 2014.
- [20] P. Bernard, L. Praly, V. Andrieu, Observers for a non-Lipschitz triangular form, *Automatica*, vol. 82, pp. 301-313, 2017.

Contribution of Individual Authors to the Creation of a Scientific Article (Ghostwriting Policy)

- Ali Bouklata: Writing, Conceptualization, methodology and software.
- Mohammed Benyassi and Adil Brouri: Project administration, Supervision and formal analysis.
- Hafid Oubouaddi and Chaima Abdelaali: Writing - review & editing.

Sources of Funding for Research Presented in a Scientific Article or Scientific Article Itself

No funding was received for conducting this study.

Conflict of Interest

The authors have no conflicts of interest to declare.

Creative Commons Attribution License 4.0 (Attribution 4.0 International, CC BY 4.0)

This article is published under the terms of the Creative Commons Attribution License 4.0
https://creativecommons.org/licenses/by/4.0/deed.en_US